JOURNAL OF THERMOPHYSICS AND HEAT TRANSFER
Vol. 6, No. 4, Oct.–Dec. 1992

Visualization of a Solidification Process in Microgravity

A. Iwasaki,* S. Hosokawa,† I. Kudo,† and M. Tanimoto*
Electrotechnical Laboratory, Umezono, Tsukuba, Ibaraki 305, Japan
H. Sakurai,‡ Y. Arai,‡ T. Watanabe,‡ and S. Kawai‡
Ishikawajima-Harima Heavy Industry, Otemachi, Chiyoda, Tokyo 100, Japan
and
M. Ishikawa§ and S. Kamei§
Mitsubishi Research Institute, Otemachi, Chiyoda, Tokyo 100, Japan

Using a polarization microscopy and interferometry, we have visualized the process of the advancing interface and the adjacent region of the fluid during unidirectional solidification on a sounding rocket, and compared it with that on the ground. Liquid-crystal material was used, and the phase transitions of both isotropic-nematic and nematic-solid were investigated. On the isotropic-nematic interface, some wavy patterns were observed and the existence of different mechanisms for each gravity level was identified. In front of the nematic-solid interface, microconvection, which was recognized on the ground, disappeared under the microgravity condition. We discuss the effect of gravity on thermal transport and phase transition using a liquid-crystal material as a unique model material.

Introduction

SINCE much concern has been focused on material processing utilizing buoyancy-free and sedimentation-free conditions, solidification has been investigated by using various spacecrafts in microgravity.[1] To put these merits to practical use, it is important to understand the physical phenomena well. In most experiments on solidification in microgravity, samples were processed in the space environment and analyzed on the ground after the recovery. As a result, we could only speculate on the minute phenomena occurring during the process. To grasp dynamic physical phenomena of a phase transition and fluid behavior, the importance of in-situ observation with a schlieren technique[2] and interferometry[3,4] has increased. Very few results, however, have been reported concerning in-situ observation of the above processing on a sounding rocket, because the mechanical condition during the launch is intolerable for precise optical components. We have developed an observation system that can endure the launching environment.

The major objective of this experiment is to observe the advancing front of the crystal and the effect of convection during the solidification. Biphenyl liquid-crystal material, which shows two thermotropic phase transitions and has unique characteristics, is used as a transparent model material. The nematic phase, which has the orientational order and characteristics of a mesophase, is suitable for this purpose. When the crystal grows into a nematic domain, the fluid motion and the nematic structure must affect the growth phenomena.

It is also interesting to observe an isotropic-nematic interface with a little latent heat, about which Ostwald et al.[5] indicated the occurrence of an instability related to the nematic phase. They explained that this instability, observed between two parallel glass plates with thickness of 30 μm and its critical velocity decreased for thicker samples, was caused by molecular ordering and wetting. Because both phases have fluidity and the nematic one is a little heavier, it is expected that the sedimentation will be serious at a large cell gap on the ground. Therefore, it is advantageous to observe the behavior of this instability without sedimentation under the microgravity condition.

This paper describes the results of the microgravity experiment on board MASER IV, a Swedish sounding rocket which was launched in March of 1990.

Substance Selection

A nematic liquid-crystal material changes phase in multisteps because of its anisotropy.[6]

$$\text{solid}\text{--}(T_m)\text{-}\rightarrow\text{liquid crystal}\text{--}(T_c)\text{-}\rightarrow\text{isotropic liquid}$$
(nematic phase)

Here, T_m denotes a melting point where the order of the molecular mass-center position is lost. T_c denotes a clearing point where the order of the molecular axis arrangement is lost. A nematic phase is a fluid state characterized with birefringence and light-scattering due to molecular arrangement. In a domain, molecules are aligned in one direction but are mobile in the molecular axis direction. A liquid-crystal phase, namely, a nematic phase here, is an intermediate phase between solid and isotropic liquid. We selected 4-cyano-4′-5-alkoxy-biphenyl (5OCB or M15 of BDH Ltd.) that was chemically stable in the temperature range of this experiment. Figure 1 shows the result of the differential scanning calorimeter (DSC) analysis, where T_m is 48°C and T_c is 68°C. It shows that the nematic phase supercools at a temperature about 30°C lower than the melting temperature in the cooling process (cooling rate: 10 deg/min). Most of the latent heat is consumed at T_m, while the isotropic-nematic transition is weakly first order with much smaller latent heat.[5,6] The latent heat of the isotropic-nematic transition is 0.2 kcal/mol and that of the nematic-solid transition is 6.9 kcal/mol. Judging from the Jackson parameter,[7] which indicates the roughness of the interface, it is expected that the isotropic-nematic interface is subject to perturbation; by contrast, the nematic-solid one grows with a faceted surface.

The nematic-solid interface was observed under a microscope in an isothermal condition. To initiate the crystal growth, the nucleus was inserted into the cell containing a sample with the thickness of 0.1 mm. The preliminary test results indicated

Received Dec. 19, 1990; revision received Oct. 2, 1991; accepted for publication Oct. 4, 1991.

*Researcher, Space Technology Section.
†Researcher, Space Technology Section. Member AIAA.
‡Researcher, Space Development Division.
§Researcher, Frontier Science Institute.

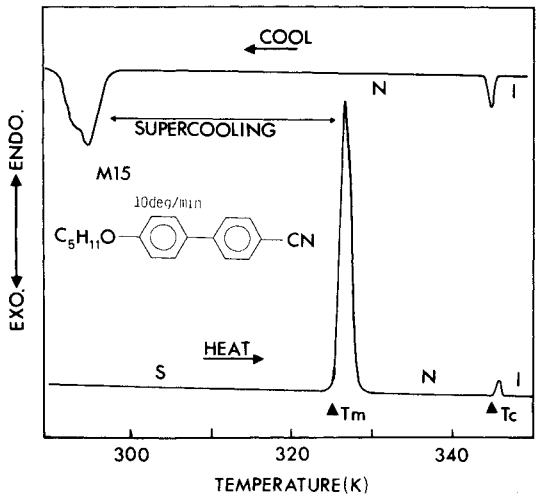

Fig. 1 Differential scanning calorimeter traces of 4-cyano-4′-5-alkoxy-biphenyl. Peaks during heating correspond to endothermic process, and reversed peaks during cooling to exothermic process. Perkin-Elmer DSC-2; scanning rate = 10°C/min; I, N, and S denote isotropic, nematic, and solid, respectively.

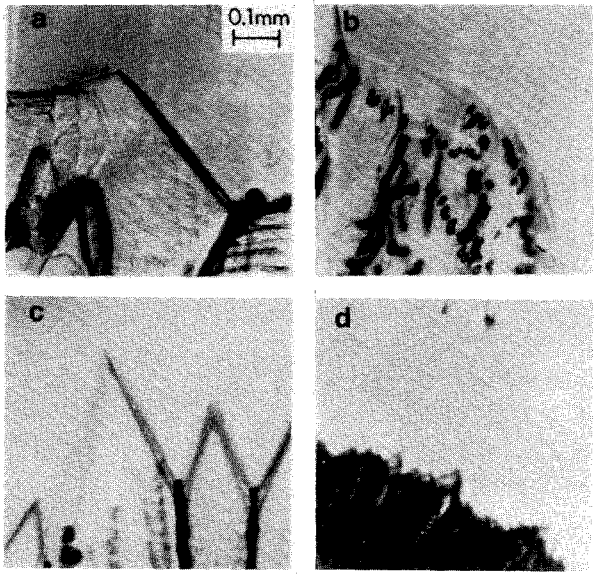

Fig. 2 Microscopic view of the nematic-solid interface. A half-vertical angle of crystal varies with temperature. The environmental temperature is a) 43°C, b) 40°C, c) 35°C, and d) 25°C, respectively.

that the growth form varied with the degree of supercooling. Figure 2 shows the typical morphologies of crystals with different environmental temperatures. Near the melting temperature, the interface advanced with a flat crystal face. When the environment temperature was decreased, the vertical angle of the crystal form changed to 116.6 deg, as shown in Fig. 2a. Around 40°C, it changed to 45 deg, as shown in Fig. 2c. The growth velocity increased when the environmental temperature was decreased. The growth velocity was 4.5, 14, and 23 mm/min for Figs. 2b, 2c, and 2d, respectively. Hill-and-valley structures were a mechanism of this growth, and the growth face changed with supercooling.

Experimental Setup

For the in-situ observation on the sounding rocket, we used a polarization microscope and a two-beam interferometer (Fig. 3). Interferometry is suitable for the visualization of the two-dimensional distribution of the refractive index, which is correlated to the temperature field. A He-Ne laser beam (linearly polarized: 1 mW) was collimated to a parallel beam of 10 mm

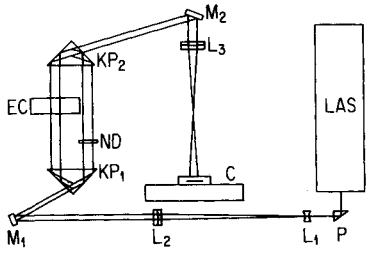

Fig. 3 In-situ observation system. LAS, laser; P, prism; L, lens; M, mirror; KP, Koester prism; ND, neutral-density filter; EC, experimental cell; C, CCD video camera.

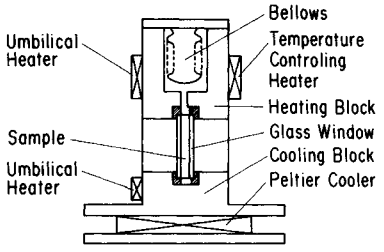

Fig. 4 Configuration of the experimental cell.

in diameter. A pair of Koester prisms were installed to split the incident laser beam into two beams and recombine them to obtain interference fringes. In this optical system, we used double-mirror reflection, which was especially effective in suppressing the influence of the vibration at the launch. The probe beam, which advanced in a fixed direction independent of the prism position, passed through the sample and interfered with the reference beam. The image was screened on a CCD video camera and recorded on an 8-mm video recorder. The range of the image was 6 mm (vertical) × 8 mm (horizontal), covering about $\frac{2}{3}$ of the field of view of the experimental cell. The resolution of the camera was more than 350 lines (vertical) x 280 lines (horizontal), which provided a spatial resolution of less than 0.1 mm. To minimize shock from the rocket, the baseplate, on which the optical components were fixed, was insulated from the rocket structure by vibration-absorbing rubber. After the vibration test, it was confirmed that the flight model functioned properly. The spectrum density of the random vibration was set at 0.1 g^2/Hz in the frequency range of 20–2000 Hz. The model was designed to endure the acceleration level of 12.7 g_{rms} during the launch.

Figure 4 shows the configuration of an experimental cell. A liquid-crystal material was enclosed in a fused-quartz cell with inner dimensions of 13 mm (height) x 15 mm (width) x 2 mm (thickness), which was assembled between a heating block and a cooling block. The sample was melted in the vacuum chamber to degas impurities, and then poured into the cell. Umbilical heaters at each block were used to melt the contained sample before liftoff. The temperature of the cooling block, which was controlled by a Peltier cooler, was measured by platinum resistance thermosensors. For heat rejection from the hotter side of the Peltier cooler, a thermal storage material was used to maintain the temperature at 28°C. A bellows was utilized in the heating block to absorb any volume change of the medium in the cell. A temperature gradient was produced between those two blocks. Because molecules in a nematic phase interacted with polished impressions on a quartz surface, the inner surface of the cell was treated with polyimide and rubbed in one direction in order to align the molecules parallel to the direction of the temperature gradient. The polarization of the laser beam was perpendicular to the molecules, which was the ordinary direction. Capillary holes were perforated in the cooling block to seed a crystal, which made a nucleus at about 25°C on the ground.

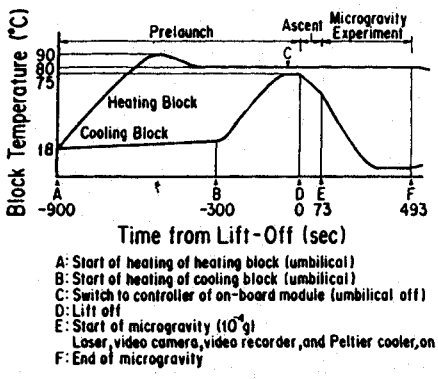

Fig. 5 Experimental sequence and temperature profile of the experimental cell.

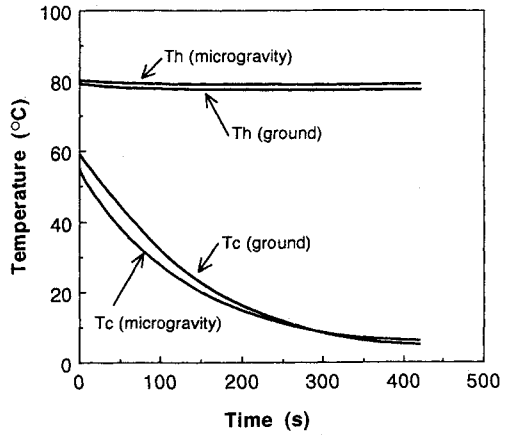

Fig. 6 Temperature profile of the heating and cooling block.

Because the flight experiment was conducted in the vacuum environment of about 10^{-2} Pa, we carried out the ground-based test in the vacuum condition. The vacuum condition was effective in reducing the heat dissipation from the outer surface of the quartz cell due to the convection of air. It also had an advantage of avoiding the fluctuation of air in the light path of the interferometer, thus enabling stable observation.

Figure 5 shows the control sequence. Before the launch, electric power was supplied from the ground support equipment. The model material was melted at first by heating both the heating block and the cooling block. The temperature of the heating block was kept at 80°C through the end of the space experiment. After the launch, an internal controller turned on the battery to supply power to the system. The cooling block was chilled down naturally during the launch period (72 s). After receiving the microgravity signal, the monitor system was turned on. The Peltier cooler began to extract heat from the cooling block with a constant current. Temperatures of the two blocks, applied current and voltage of the heater and cooler were transmitted to the ground by the telemetry system. The duration of the microgravity experiment was 438 s with a gravity level of less than 10^{-4} g. The ground-based experiment was conducted in the same sequence. To make the system stable to the thermal convection on the ground, the sample was cooled from the bottom. The dimensions of the setup were 438 mm (diam) x 460 mm (longitude), and the total weight was about 26.6 kg, excluding the hull.

Results and Discussion

Temperature Profile

Figure 6 shows the temperature profile for the heating block and the cooling block both on the ground and in microgravity. On the rocket experiment, because the air around the setup lowered the temperature of the cooler block, its profile was about 5°C lower than that of the ground-based experiment at the initiation of the experiment, which brought about the cooling process on the sounding rocket about 15 s in advance.

Interface Between Isotropic and Nematic

Figure 7 shows the position of the isotropic-nematic interface from the bottom. Because the latent heat discharged during the isotropic-nematic transition was small, the growth rate was faster than that during the nematic-solid process. We did not recognize the effect of microgravity on the growth rate, which could be calculated from the slopes of Fig. 7. Because adhesive growth was superior in the mechanism of this process, this interface hardly showed supercooling; thus, we judged the interface to be an isothermal line of the clearing point (T_c = 68°C) in the temperature gradient.

Figure 8 shows the photograph of the isotropic-nematic interface. The width of a meniscus in the vertical direction of the sample was large on the ground (Fig. 8a). The upper part of the meniscus mainly resulted from the process occurring on the cell surface. The position of the advancing meniscus depended on the temperature gradient in the cell. A wavy pattern in the horizontal direction was observed on the bottom of the meniscus. The wavelength of these patterns was about 0.2 mm, while the amplitude was small. The molecules in the nematic phase, which wetted the cell surface, gathered and sank due to gravitational force and generated a wavy pattern in the horizontal direction. Schematic representation of the meniscus in the vertical plane is shown in the lower part of Fig. 8, where the isotropic phase bulged into the nematic phase. It was found that the meniscus was observed when the growth rate was faster than 0.01 mm/s, and that as the growth rate increased, the width of the meniscus in the vertical direction became greater.

In the rocket experiment (Fig. 8b), the interface line showed a parabolic curve because the de-spinning of the rocket just

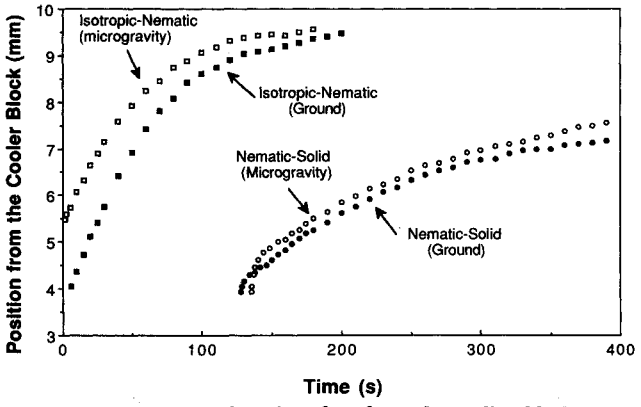

Fig. 7 Position of the interface from the cooling block.

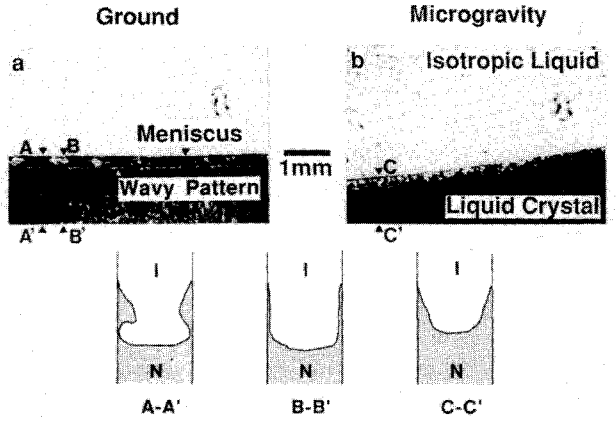

Fig. 8 Photograph of the isotropic-nematic interface: a) on the ground, and b) in microgravity.

before the microgravity signal caused an acceleration around the major axis. The curved line recovered within the next 25 s; that is, the interface advanced perpendicular to the temperature gradient. By comparing Fig. 8b with 8a, we found that the width of the meniscus in the vertical direction was 0.1 mm in microgravity, but 0.3 mm on the ground. The nematic phase did not sink in microgravity, and a small wave in the horizontal direction about 0.1 mm in wavelength was observed. This wavy pattern was due to the fluctuation in the meniscus. From the successive images, we observed the wavy pattern fused and then collapsed. Bechhoefer[8] reported that the nematic phase wetted the glass plate treated with silane, where the molecule was arranged perpendicular to the glass plate. In our case, although the molecular direction was different, the same phenomena was observed. The meniscus was caused in the process of arrangement of molecules on the glass surface. In microgravity, the wavy pattern was supposed to be determined by the buckling force and the hydrodynamic force.[8] But it was difficult to specify the main driving force because the cell gap was very large compared to the case of Bechhoefer's[8] experiment and the situation was more complicated. On the ground, the meniscus was easily buckled due to the gravitational force, and the wavy pattern was made by the nematic phase on the glass surface, which dropped on the bottom of the meniscus.

The domains were too small to be observed in this system at the temperature just below T_c. However, as the temperature decreased, disclination lines (the boundaries of domains) interacted, and domains fused to be about 3 mm in size, which varied with temperature condition and growth rate. Within a domain, the interference fringes were continuous. Because the alignment coating was somewhat damaged, the size of each domain was small in the rocket experiment.

Interface Between Nematic and Solid

When the temperature of the cooling block decreased to about 25°C, which was 23°C below the melting point, solidification started on the ground. Figure 7 shows the position of this interface. Although the temperature of the cooling block was at least 3°C lower in microgravity, the start of solidification was slightly delayed. Main causes for the delay were considered to be the differences in the heat conduction and the lower nucleation rate. Similar delay of solidification onset under the reduced gravity condition in the case of succinonitrile was reported.[4]

The nematic-solid interface advanced quite rapidly into the supercooled region and the size of the grown crystal was small due to the large extent of supercooling. The growth rate exceeded 10 mm/min at maximum, which was consistent with the result in the isothermal condition. Because the temperature of the nematic phase around the cooling block was lower in microgravity, the solidification rate was faster. The growth rate decreased during the next 10 s after that due to the accumulation of latent heat at the interface. It formed a temperature-reversed layer in front of the interface when the solid phase advanced into the supercooled liquid.[4] Because we adopted an infinite fringe method, it was difficult to observe the thickness of the layer. The growth rate oscillated about 50 s after the start of the solidification, which was larger in microgravity. The variation of the growth rate depended on both the release of latent heat and its diffusion away from the interface.

Figures 9a and 9b show the nematic-solid interface at 210 s after the cooling started. In this process, the heat transfer of latent heat in the temperature gradient limited the solidification rate. The crystal was about 0.25 mm in size and showed the same form as Fig. 2c. Interferometric fringes near the interface moved parallel to the interface at equal spaces, which suggested that the temperature of the crystal was kept almost constant. We could observe the movement of disclination lines on the ground, which was caused by the convection around the interface even in the stable system of temperature gradient. As a result, the form of the interface was disturbed. By contrast, the convection was restrained in microgravity and the faceted interface was clear, as shown in the magnified picture. To clarify the fluid motion in front of the interface, the differences between two images at small intervals (0.33 s) were enhanced by means of a video processor (Figs. 9c and 9d, which corresponded to Figs. 9a and 9b, respectively). The bright part in front of the interface on the ground data represented the changes in the nematic phase but did not extend over the entire liquid region (Fig. 9c). By contrast, there existed little change in the nematic phase under the microgravity condition (Fig. 9d). The convection in this region possibly occurred for the following reasons. First, a discharge of the latent heat in the interface built up the temperature-reversed layer. Second, motion of domains was induced in the nematic phase due to temperature increases, where the nematic phase plays a role as a tracer. Third, there occurred a discharge of slightly mixed impurities. Because convection was restrained under the microgravity condition, heat transfer from the nematic side became small and the growth rate increased, as shown in Fig. 7. As the interface advanced further, the hill-and-valley structure of the interface became large in microgravity, while the structure collapsed due to the microconvection in front of the interface on the ground.

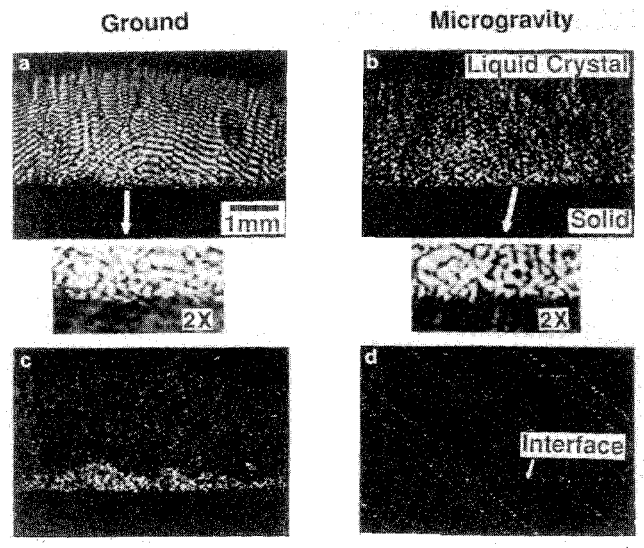

Fig. 9 Images of the nematic-solid interface: a) on the ground, b) in microgravity, c) time differential image on the ground, and d) time differential image in microgravity.

During the solidification, the disclination lines interacted with an advancing front and were sometimes drawn by the front. One possible explanation is that aligned molecules were rearranged as crystals, which caused some change in the nematic phase. Because the interface shows a wavy pattern in the case of misfit alignment, there exists the effect of the convection to alignment on the ground.

Conclusions

Using a liquid-crystal material as a model, we investigated the influence of the gravity level on the isotropic-nematic and nematic-solid interfaces. We showed that some wavy patterns were recognized at the isotropic-nematic interface with a little latent heat. In the nematic-solid interface, we visualized a microconvection around the nematic-solid interface on the ground, and showed that it was restricted under the microgravity condition and that the morphology of the interface became sharp. We also found that an interaction existed between the solid front and the nematic structure.

We have developed a sophisticated Mach-Zehnder interferometer with a double-mirror reflection technique that could endure the mechanical condition on a sounding rocket. It worked well during the experiment and was recovered on the

ground undamaged, which could make way for in-situ observation of the solidification process in the future.

Acknowledgments

This work was carried out with the aid of funds from the Mechanical Social Systems Foundation and the Society of Japanese Aerospace Companies, Inc.

References

[1]Hurle, D. T. J., Muller, G., and Nitsche, R., "Crystal Growth from the Melt," *Fluid Science and Material Science in Space*, edited by H. U. Walter, Springer-Verlag, Berlin, 1987, pp. 313–354.

[2]McCay, M. H., and McCay, T. D., "Experimental Measurement of Solutal Layers in Unidirectional Solidification," *Journal of Thermophysics and Heat Transfer*, Vol. 2, No. 3, 1988, pp. 197–202.

[3]Ecker, A., "Two-Wavelength Holographic Measurement of Temperature and Concentration During Alloy Solidification," *Journal of Thermophysics and Heat Transfer*, Vol. 2, No. 3, 1988, pp. 193–196.

[4]Iwasaki, A., Hosokawa, S., Kudo, I., Tanimoto, M., Fujita, S., and Takei, F., "Interferometric Observation of Phase-Change Phenomena Under Reduced Gravity," *Journal of Thermophysics and Heat Transfer*, Vol. 4, No. 3., 1990, pp. 410–411.

[5]Ostwald, P., Bechhoefer, J., and Libchaber, A., "Instabilities of a Moving Nematic-Isotropic Interface," *Physical Review Letters*, Vol. 58, No. 22, 1987, pp. 2318–2321.

[6]de Gennes, P. G., *The Physics of Liquid Crystals*, Oxford University Press, Oxford, England, UK, 1974.

[7]Jackson, K. A., and Hunt, J. D., "Transparent Compounds that Freeze Like Metals," *Acta Metallurica*, Vol. 13, No. 11, 1965, pp. 1212–1215.

[8]Bechhoefer, J., "Directional Solidification at the Nematic-Isotropic Interface," Ph.D. Thesis, Univ. of Chicago, Chicago, IL, 1988.